

## Electronic Supplementary Information

### Silicone-based tough hydrogels with high resilience, fast self-recovery and self-healing properties

Liqi Si<sup>a</sup>, Xiaowen Zheng<sup>a</sup>, Jun Nie<sup>a,b</sup>, Ruixue Yin<sup>c</sup>, Yujie Hua<sup>c</sup>, Xiaoqun Zhu<sup>\*a,b</sup>

<sup>a</sup>State Key Laboratory of Chemical Resource Engineering, Beijing University of Chemical Technology, Beijing 100029, China

<sup>b</sup>Changzhou Institute of Advanced Materials, Beijing University of Chemical Technology, Changzhou, Jiangsu, 213164, P. R. China

<sup>c</sup>Complex and Intelligent Research Center, School of Mechanical and Power Engineering, East China University of Science and Technology, Shanghai, P. R. China

E-mail: zhuxq@mail.buct.edu.cn

## 1. Experimental details

### 1.1 Materials and instruments

Methyltrimethoxysilane (MTMS) was purchased from TianJing HEOWNS Co., Ltd. Hydroxyethyl acrylate (HEA) was obtained from Aladdin Industrial Corporation. Photoinitiator 2-hydroxy-1-[4-(hydroxyethoxy) phenyl]-2-methyl-1-propanone (2959) was given by Tianjing Jiuri Co., Ltd. Cetyl trimethyl ammonium Bromide (CTAB) and urea were both purchased from Xilong Chemical Co., Ltd. All reagents were used as received without further purification. LED lamp used as the light source was donated by LAMPLIC Corporation (Shenzhen, Guangdong, China). The radiation intensity was measured by UV-A Radiometer (Photoelectric Instrument Factory of Beijing Normal University).

### 1.2 Hydrogel preparation

Herein, the hydrogel samples are defined as H<sub>x</sub>M<sub>y</sub>, where x and y are the molar ratio of HEA to MTMS, for example, H<sub>6</sub>M<sub>2</sub> means that the molar ratio of HEA and MTMS is 6/2. In this case, the ratio of typical formulation is MTMS: urea: CTAB = 1:1:0.04 (molar ratio) and the water content is about 55wt%. First of all, the mixture was stirring for 1h for hydrolysis. Then the solution was injected into a polytetrafluoroethylene (PTFE) mold for photopolymerization. After that, the bulk was put into an oven (80°C for 9h) for base-catalyzed gelation. The photopolymerization process

was conducted in glove box, and the scheme of preparation process of silicone/PHEA hydrogels was shown in Fig. S1.

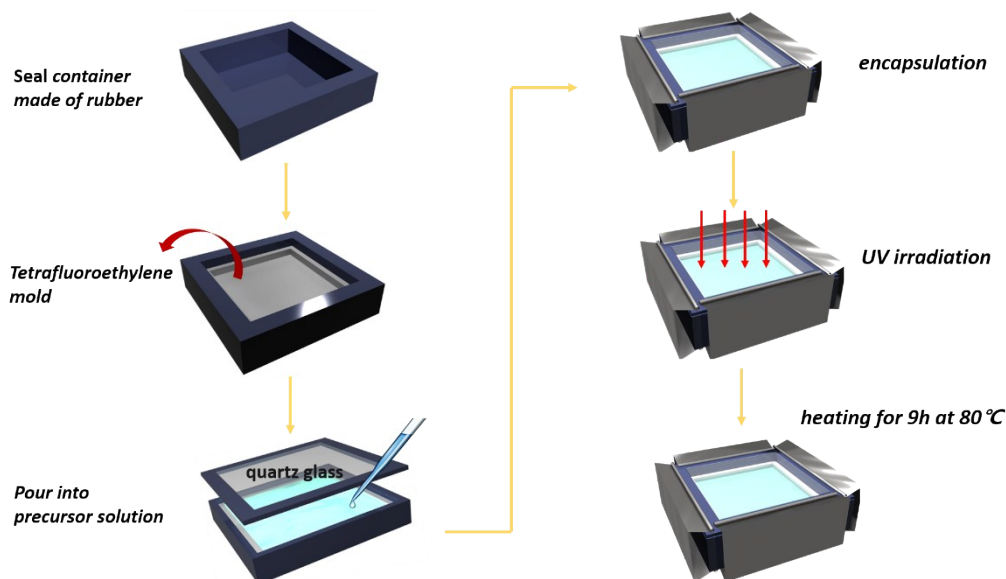


Fig. S1 The scheme of preparation process of silicone/PHEA hydrogels

## 2. Characterization

### 2.1 Mechanical properties

An Instron 3366 electronic universal testing machine (Instron Corporation, Norwood, MA) was used for mechanical testing. An Instron E1000 Fatigue testing machine (Instron Corporation, England) was used for antifatigue compression testing.

#### 2.1.1 Tensile tests

According to DIN-53504 S3, the hydrogels were cut into standard dumbbell (width: 2 mm; length: 10 mm, thickness: 2 mm). The tensile tests were carried out at room temperature with a 500-N load cell. The rate of stretch remained constant at 100 mm/min. The engineering stress ( $\sigma$ ) was calculated as  $\sigma = F/S$ , where  $S$  is sectional area of the specimen and  $F$  is the load. The engineering strain ( $\varepsilon$ ) was defined as the change in length ( $l$ ) relative to the initial gauge length ( $l_0$ ) of the specimen,  $\varepsilon = (l - l_0)/l_0 \times 100\%$ .

#### 2.1.2 Compression tests

The samples for compression tests were made for cylinder (diameter: 20mm; thickness: 13mm). The rate of compression was 5mm/min. The engineering stress ( $\sigma$ ) was calculated as  $\sigma = F/S$ ,

where  $S$  is sectional area of the specimen and  $F$  is the load. The engineering strain ( $\epsilon$ ) was defined as the change in height ( $h$ ) relative to the initial height ( $h_0$ ) of the specimen,  $\epsilon = (h - h_0)/h_0 \times 100\%$ .

### 2.1.3 Cycle loading-unloading tests

For hysteresis measurements, hydrogel samples were first stretched (or compressed) to a maximum (minimum) strain  $\epsilon_1$  and then unloaded. When the sample returning to the original length, the samples were reloaded again and stretched (or compressed) to aforementioned strain  $\epsilon_1$  with the same velocity rate as the first loading and then unloaded. The loading–unloading operations were repeatedly conducted on the same sample for 5 cycles. The rate of stretch was 100 mm/min for tensile cycle tests and 5mm/min for compressive tests. Herein, to quantitatively determine the hysteresis loop, we defined  $hr$  as the ratio of the area of the hysteresis loop ( $\Delta S$ ) to the integrated area of the loading curve ( $S_l$ ),  $hr = \Delta S/S_l$ .<sup>1</sup>

For self-recovery tests, hydrogel sample was first stretched with a certain strain  $\epsilon$  and then unloaded. The rate of stretch was 100 mm/min for tensile cycle tests. After 1min, the same process was repeated. The compression loading-unloading tests were similar to tensile tests. The rate of compression was 5mm/min for compressive tests.

### 2.1.4 Anti-fatigue compression tests

The sample for anti-fatigue compression tests was cylindrical (diameter: 20mm; thickness: 13mm). 50 cycle times were employed for studying the evolution of the samples in the program. Besides, the different frequency, 0.1HZ, 1HZ was investigated respectively for the same sample.

### 2.1.5 Tearing measurement tests (ASTM D624-00)

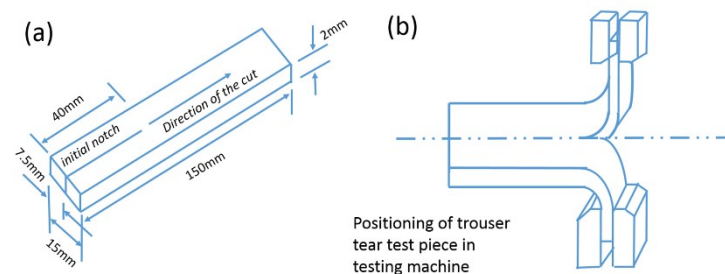


**Fig.S2** (a) Sample shape ( $w = 15$  mm,  $L = 150$  mm,  $d = 2$  mm, the length of the initial notch is 40 mm) and (b) the tearing method to measure fracture energy.

---

The fracture energies  $G$  of the hydrogel were measured by tearing tests which was performed according to ASTM D624-00 (Standard test method for tear strength of conventional vulcanized rubber and thermoplastic elastomers). The samples were cut into trousers-shaped samples (2 mm in thickness, 150 mm in length with an initial notch of 40 mm and 15 mm in width) (Fig.S2). The pulling velocity ( $V_p$ ) is 50 mm/min. The fracture energy  $G$ , defined as the energy required for creating a unit area of fracture surface in a sample, is calculated by the following equation,  $G=F_{ave}/d$ , Where  $F_{ave}$  is the average force during the tear measurement and  $d$  is the thickness of the samples.

## 2.2 ATR-IR spectrum analysis

Attenuated Total Reflectance - Infrared Radiation (ATR-IR) spectrum was recorded on Nicolet 5700 instrument (Nicolet Instrument, Thermo Company, USA) with id3 ATR accessory. Samples were prepared as dried gels membranes and were scanned against air background at wavenumbers range 4000–500  $\text{cm}^{-1}$  with resolution of 4.0  $\text{cm}^{-1}$ . The peaks area was calculated by a software omnic 32.

## 2.3 Dynamic mechanical thermal analysis (DMTA)

Dynamic mechanical thermal analysis was performed on dynamic mechanical thermal analyzer (NETZSCH 242C, Germany) at a heating rate of 5  $^{\circ}\text{C min}^{-1}$  in the range of  $-200$  to  $80^{\circ}\text{C}$  with the sheet of 10 mm  $\times$  5 mm  $\times$  1 mm. The glass transition temperature ( $T_g$ ) was defined as the peak of  $\tan\delta$  curve.

## 2.4 SEM morphology analysis

The fracture surface morphology of the freezing dried hydrogel was observed by using Hitachi S-4700 scanning electron microscope (SEM) (Hitachi Company, Japan). Its accelerating voltage was 20 kV. Before tests, the samples were mounted on metal stubs using a double-sided adhesive tape and vacuum-coated with gold sputtering layer prior to examination. Microstructure of the samples was analyzed from the SEM images by using Image J analysis software (Image J, National Institutes of Health, USA).

---

## **2.5 In vitro cytotoxicity and compatibility of hydrogels**

### **2.5.1 Methylthiazolyldiphenyl-tetrazolium bromide (MTT) assay**

The cytotoxicity of the hydrogels was evaluated based on a procedure adapted from the ISO10993-5 standard test method.<sup>2</sup> Mouse fibroblast cell line (L929) was cultured on a 96-well tissue culture plates (100 $\mu$ L/well; Cellstar) at  $1 \times 10^5$  cells/mL in DMEM (Dulbecco's modified Eagle's medium; Sigma- Aldrich, USA) containing 10% fetal bovine serum (FBS, Sigma-Aldrich, USA), and then incubated at 37°C in 5% CO<sub>2</sub> for 4 h. The viabilities of cells were determined by the MTT (3-[4,-dimethylthiazol-2-yl]-2, 5-diphenyltetrazolium bromide; thiazolyl blue) assay. The level of the reduction of MTT into formazan can reflect the level of cell metabolism. For the MTT assay, the hydrogels were sterilized with highly compressed steam for 15 min. For reference purposes, cells were seeded to medium containing 0.64% phenol (positive control) and a fresh culture medium (negative control) under the same seeding conditions, respectively. The presence of cytotoxic leachates in the extract was verified by MTT assay after incubating the cells with the extract for 24, 48 and 72 h. In the assay, fresh media containing 10% of MTT replaced the medium and the plate was incubated at 37°C in CO<sub>2</sub> incubator for 4 h. After that, the unreacted dye was removed by aspiration. The produced formazan crystals were dissolved in DMSO (100  $\mu$ L/well). The optical density of the formazan solution was detected by an ELISA reader (Multiscan MK3, Labsystem Co. Finland) at 490 nm.

### **2.5.2 Cell culture and adhesion**

Mouse fibroblast cell line (L929) was selected for the biological assays in order to evaluate the effect of hydrogels on cell culture, adhesion, and proliferation.<sup>3</sup>The hydrogels were sterilized, rinsed three times with sterile phosphate buffer solution (PBS), then transferred to individual 96-well tissue culture plates. Aliquots (1 mL) of L929 cells suspension with  $1.5 \times 10^4$  cells/mL were seeded on the hydrogels. After 24 h of culture, cellular constructs were harvested, rinsed twice with PBS to remove non-adherent cells.

---

## 3. Results and discussion

### 3.1 The influence of the content of CTAB on the appearance and mechanical property of the hydrogel

The silicone/PHEA hydrogels had obvious phase separation without surfactant CTAB. As shown in Fig. S3a, the samples became transparent with increasing amount of CTAB. However, the excess CTAB would induce the gels opacity again. The different quantity of CTAB was a little influence on mechanical properties of the hydrogels (Fig. S3b, due to the good compatibility of the dual polymer networks).

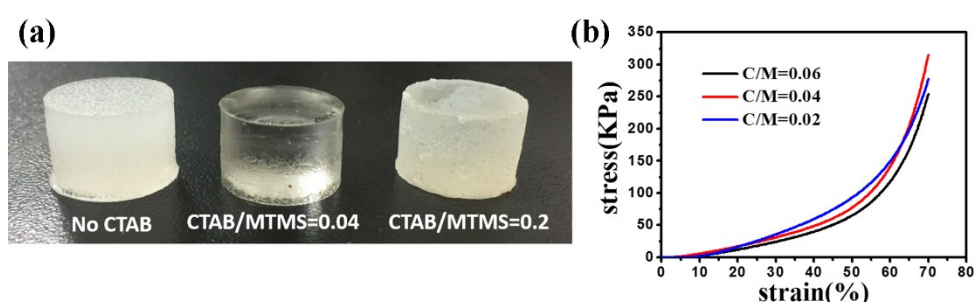


**Fig.S3** (a) The image of H6M2 samples with different content of CTAB (the molar ratio between MTMS and CTAB); (b) Compressive stress-strain curves of hydrogels with different content of CTAB.

### 3.2 The ATR-IR spectrum analysis

Fig. S4a shows the ATR-IR spectra of silicone/HEA hydrogel in  $800\text{-}1400\text{ cm}^{-1}$ . The band at  $918\text{ cm}^{-1}$  is associated with the stretching of Si-OH groups, and the results also show the existence of both Si-O-Si groups ( $1095\text{ cm}^{-1}$ ) and Si-O-C groups ( $1030\text{ cm}^{-1}$ ) in silicone/PHEA hydrogel, suggesting the formation of Si-O-C bonds and the occurrence of a condensation reaction between PHEA and MTMS. Meanwhile, the top surface, cross section and bottom surface of the hydrogel was chosen and investigated by ATR-IR (Fig.S4b), we could find the IR spectra are same for these surface. It demonstrated the hydrogel was uniform.

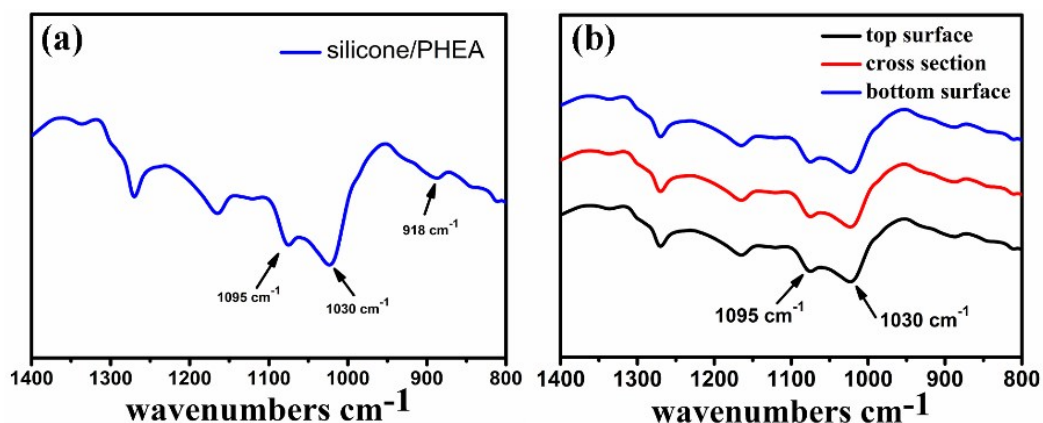


**Fig.S4** (a) The ATR-IR spectra of silicone/HEA hydrogel; (b) The ATR-IR spectra of top surface, cross section, bottom surface of silicone/PHEA hydrogel

### 3.3 Dynamic mechanical thermal analysis

From the  $\tan \delta$  - temperature curve of DMTA, we could see there was only one peak from -200 to 80 degree (Fig. S5). It showed that the silicone/PHEA hydrogel had only one glass transition temperature which also demonstrated the hydrogel was uniform and the two polymer networks were well compatible.

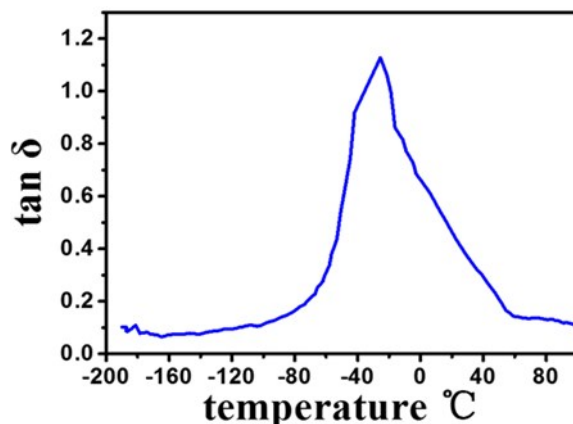


**Fig. S5** The  $\tan \delta$  - temperature curve of silicone/PHEA hydrogel

### 3.4 The microstructure of silicone/PHEA hydrogels

The microstructure of silicone/PHEA hydrogel and silicone hydrogel was investigated by scanning electron microscope (SEM). As shown in Fig. S6a, the whole network of silicone/PHEA hydrogel was homogeneous, and there was no particle, which demonstrates that MTMS did not form nanoparticles. While, the silicone hydrogel was composed of particles and the particles are discontinuous (Fig. S6b).

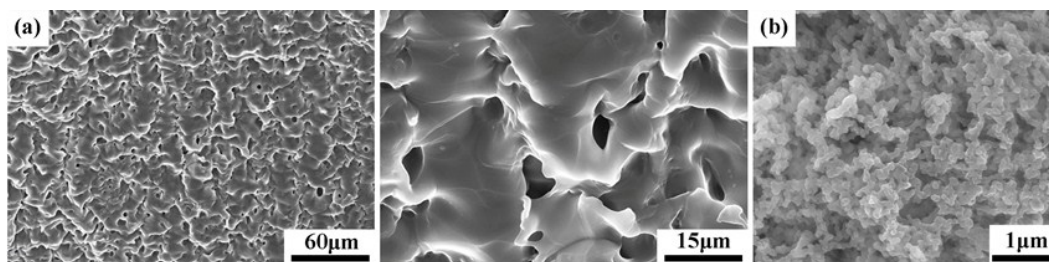


**Fig. S6** The SEM images of the microstructure of silicone/PHEA hydrogel (a) and silicone gel (b)

### 3.5 The images of silicone gels, PHEA gels

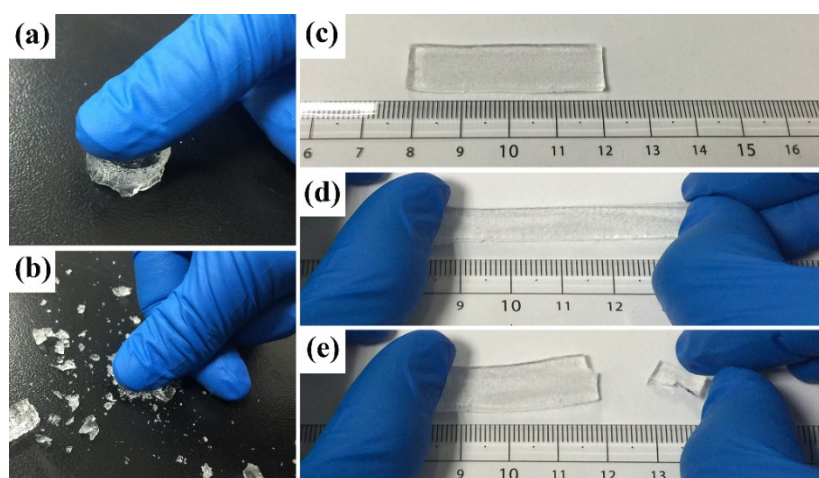


**Fig.S7** (a, b) The silicone gel was very brittle which was crushed easily by finger without PHEA; (c, d, e) The PHEA gel was soft without crosslinker. Both of them could not be tested by mechanical experiments.

### 3.6 The images of silicone/PHEA hydrogels

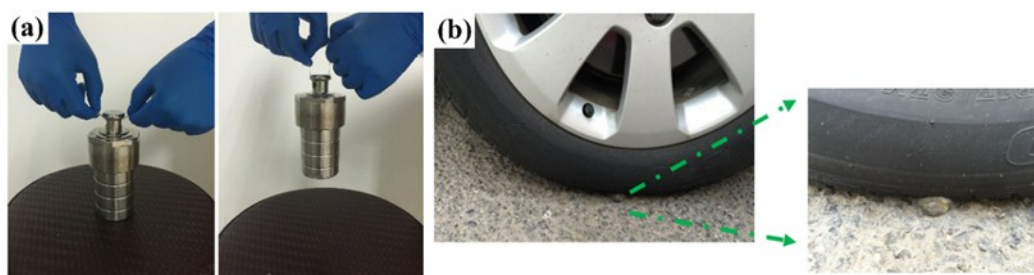
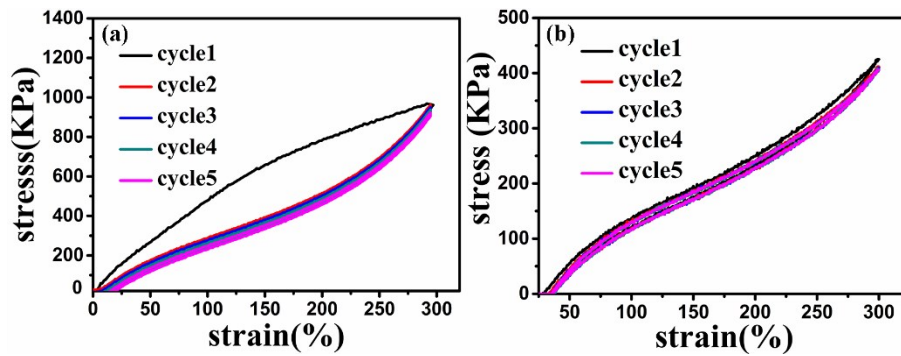


**Fig.S8** (a) A steel block with a weight of 1.6 kg could be lifted up by the prepared H6M2 gel with 1.5mm thickness and 4mm width; (b) Images of the H6M2 sample bore a series of crashing by a car for 30 times without failure.



### 3.7 The tensile cycle tests for five runs of H5M2 hydrogel

The typical successive loading–unloading tensile tests for five runs of H5M2 hydrogel was conducted, due to higher modulus. However, as shown in Fig. S9, the resilient of the H5M2 hydrogel was not as well as the H6M2 hydrogel. A little more PHEA in the network (H6M2) may decrease the crosslinking density of the silicone which gives the good ductility to the hydrogel

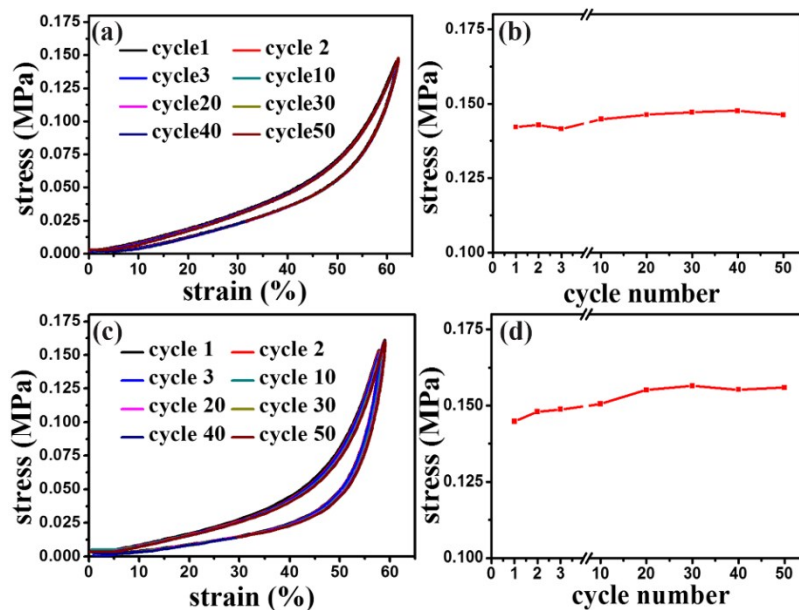


(H6M2).

Fig.S9 The typical successive loading–unloading tensile tests for five runs of H5M2 (a) and H6M2 (b) hydrogel at 300% strain

### 3.8 Anti-fatigue behavior of silicone/PHEA hydrogels

To further investigate the anti-fatigue behavior of the hydrogels, the compression loading–unloading with 50 cycles tests at 60% strain was performed. As shown in Fig. S10, even after 50 cycles, the stress of hydrogels still increased. As the frequency increase, the stress increased more.



---

Fig.S10 (a, b) The successive loading–unloading compression tests for 50 runs (0.1HZ); (c, d)  
The successive loading–unloading compression tests for 50 runs (1HZ).

### 3.9 In vitro cytotoxicity and compatibility

In Fig. S11a, for hydrogels, the average absorbance values were lower than that of the negative control, but the cell relative proliferation rate still reached above 95% of that of the negative control. This indicated that the hydrogels were less toxic to L929 cells.

The compatibility between silicone/PHEA hydrogels and cells was observed by fluorescence microscope (Fig. S11b) which showed the L929 cells could attach on the surface of hydrogels after 48 h culture. The fluorescent images showed that the attached cells exhibited the spindle shape, typical of active fibroblastic cells, and normal cell nucleus morphology.

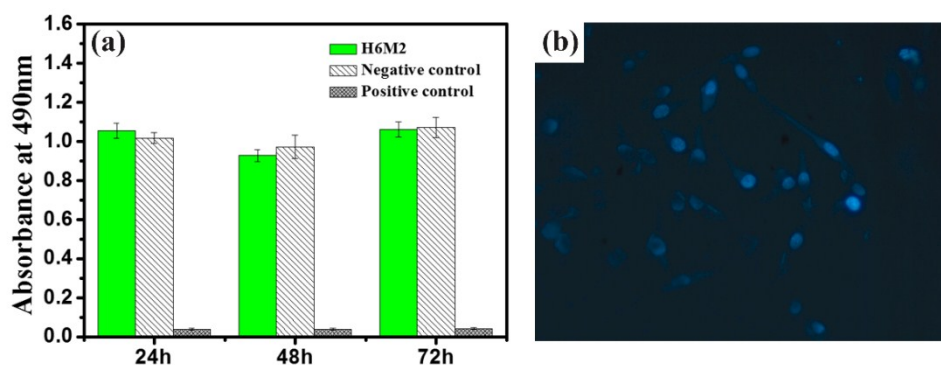


Fig.S11 (a) MTT test of L929 cell seeded on the hydrogels; (b) Fluorescence microscope images of L929 cell seeded on the hydrogels

### Reference

1. C. C. He, Z. W. Zheng, D. Z. J.Q. Liu, J. Ouyang and H. I. Wang, *Soft Matter*, 2013, 9, 2837.
2. (a)Y. S. Zhou, D. Z. Yang, X. M. Chen, Q. Xu, F. Lu and J. Nie, *Biomacromolecules*, 2008, 9, 349;(b) J. -F. Zhang, D. -Z. Yang, F. Xu, Z. -P Zhang, R.-X Yin and J. Nie, *macromolecules*, 2009, 42, 5278.
3. A. M. Costa, and J. F. Mano, *Chem Commun*, 2015, 51, 15673.